Science and Technology Indonesia
e-ISSN:2580-4391 p-ISSN:2580-4405
Vol. 11, No. 1, January 2026

Research Paper

Synthesis of NiO Nanoparticles as a Catalyst in Transesterification Reaction from Used Cooking Oil for Biodiesel Production

Hasri[1*], Suriati Eka Putri[1], Satria Putra Jaya Negara[1], Nur Afni[2], Fadil Anwar[2]

[1]*Department of Chemistry, Faculty of Mathematics and Natural Science, Universitas Negeri Makassar, Makassar, South Sulawesi, 90224, Indonesia*
[2]*Students of Chemistry Department, Faculty of Mathematics and Natural Science, Universitas Negeri Makassar, Makassar, South Sulawesi, 90224, Indonesia*
***Corresponding author**: hasriu@unm.ac.id

Abstract
This study aims to synthesize and characterize nickel oxide (NiO) nanoparticles as heterogeneous catalysts for biodiesel production from used cooking oil through transesterification. The synthesis was conducted using the sol-gel method with $NiCl_2 \cdot 6H_2O$ as a precursor and NaOH as an alkaline agent. Characterizations were then performed using Particle Size Analysis (PSA), X-ray Diffraction (XRD), Scanning Electron Microscopy with Energy Dispersive Spectroscopy (SEM-EDS), and Specific Surface Area (SAA) analysis. The PSA results showed that the samples had an average particle size of 37.0 nm with a narrow distribution (PDI = 0.010). XRD confirmed a cubic crystal structure corresponding to JCPDS No. 47-1049, while SEM images showed revealed uniform spherical morphology. In addition, EDS analysis verified the composition of Ni and O as the main elements. The SAA of 489.26 m^2/g showed high catalytic activity potential. Catalyst performance tests with methanol-to-oil molar ratios of 1:3, 1:6, and 1:9 showed the highest biodiesel yield of 97.79% at a 1:9 ratio. The produced biodiesel met the Indonesian National Standard (SNI 7182:2015) with a density of 0.86–0.89 g/mL, acid number of 0.40–0.50 mg KOH/g, iodine number of 67.73–93.13 g I_2/100 g, and cetane number of 76.87–114.86. GC-MS analysis showed methyl ester chains between C15–C21, confirming compliance with APEC standards. Based on these results, NiO nanoparticles showed high efficiency as an eco-friendly heterogeneous catalyst for biodiesel production.

Keywords
Biodiesel, Heterogeneous Catalysts, Used Cooking Oil, NiO Nanoparticles, Transesterification

Received: 18 September 2025, Accepted: 25 November 2025
https://doi.org/10.26554/sti.2026.11.1.280-287

1. INTRODUCTION

The global energy crisis due to the limitation of fossil resources has facilitated the search for alternative energy that is sustainable and environmentally friendly. One potential solution is biodiesel, a biofuel that can be produced from various vegetable oils and oil waste such as used cooking oil (Monika et al., 2023). Apart from being a cheap raw material, the use of used cooking oil also contributes to the management of household waste which is an inedible raw material (not eaten) (Buchori et al., 2024; Oladipo et al., 2025).

According to previous studies, the main process in biodiesel production is transesterification, which converts triglycerides in oil into methyl esters using alcohols and catalysts (Naseef and Tulaimat, 2025; Wan Osman et al., 2024). However, the use of homogeneous catalysts, such as KOH or NaOH, has several drawbacks, including being difficult to separate from the product, causing soap formation, and lowering the purity of biodiesel. Therefore, the development of heterogeneous catalysts is an alternative solution (Anekwe et al., 2025; Sales et al., 2020).

Nickel oxide (NiO) nanoparticles are a promising heterogeneous catalyst due to their high surface area, thermal stability, and good catalytic activity (Al-Fakeh et al., 2025; Bikbashev et al., 2024; Dey and Mehta, 2020; Pratiwi et al., 2024). The sol-gel method is used in the synthesis because it produces particles with uniform morphology and nanosize at relatively low temperatures (Borlaf and Moreno, 2021; Saputra et al., 2024).

The innovation in the current study is not only reflected in the innovation of the NiO nanocatalyst synthesis method, but also in its strategic application in processing domestic waste, namely used cooking oil, as a source of renewable energy raw materials. This approach strengthens the contribution of research to the development of alternative energy technologies that are economically efficient, environmentally friendly, and based on the utilization of local resource potential.

This study aims to synthesize NiO nanoparticles using the sol-gel method, characterize them comprehensively, and test

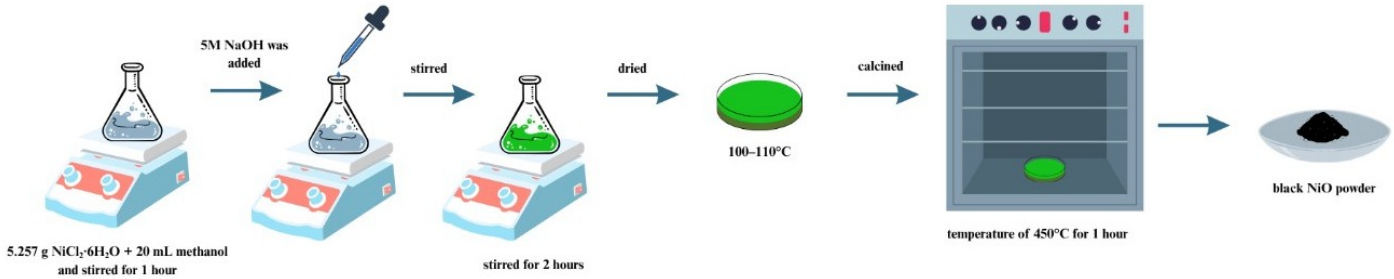

Figure 1. NiO Catalyst Working Scheme

their performance as a catalyst in the process of transesterification of used cooking oil into biodiesel with quality according to Indonesian National Standards (SNI). Previous studies have reported the use of heterogeneous catalysts in biodiesel production, including several metal oxides such as CaO, ZnO, and TiO_2. However, only a few studies have focused on the application of NiO nanoparticles, specifically those synthesized via the sol–gel method, which offers better control of particle size, morphology, and surface area. There is also limited information on the use of NiO nanocatalysts for the direct conversion of used cooking oil, a low-cost domestic waste, into biodiesel that meets both national (SNI 7182:2015) and international (APEC) standards. Therefore, this study aims to synthesize and characterize NiO nanoparticles prepared by the sol–gel method as well as evaluate their catalytic performance in biodiesel production from used cooking oil. The results are expected to show the superior physicochemical properties of NiO nanocatalysts as well as their potential as an environmentally friendly and efficient catalyst for sustainable biodiesel production.

2. EXPERIMENTAL SECTION

2.1 Materials

The materials used in this study included nickel (II) chloride hexahydrate ($NiCl_2{\cdot}6H_2O$), sodium hydroxide (NaOH), methanol (CH_3OH), used cooking oil, Wijs reagent/iodine monochloride (ICl), sodium thiosulfate ($Na_2S_2O_3$), potassium iodide (KI), alcohol 95% (C_2H_5OH), and PP indicator ($C_{20}H_{14}O_4$).

Equipment used included X-ray Diffraction (XRD, MiniFlex II Rigaku), Scanning Electron Microscopy equipped with Energy Dispersive Spectroscopy (SEM–EDS, Tescan LMU), Surface Area Analyzer (SAA, Quantachrome Novatouch LX4), Particle Size Analyzer (PSA, NKT), and biodiesel characterization tools using a pycnometer and Gas Chromatography (GC–MS, Ultra Shimadzu).

2.2 Methods

The used cooking oil was obtained from household sources, filtered to remove food residues and solid impurities, and heated to eliminate moisture. After cooling to room temperature, the pretreated oil was stored in a clean, sealed container for further experiments in the transesterification process.

NiO nanoparticles were synthesized using the sol-gel method. A total of 5.257 g of $NiCl_2{\cdot}6H_2O$ was dissolved in 20 mL of methanol and stirred for 1 hour at room temperature. A 5 M NaOH solution was added dropwise, then stirred for 2 hours until a green gel was formed. The gel was dried at 100 to 110°C, and calcined at 450°C for 1 hour to obtain NiO black powder (Figure 1) (Hasson and Alsammarraie, 2022).

Catalyst Characterization was carried out using Particle Size Analyzer (PSA), X-Ray Diffraction (XRD), Scanning Electron Microscopy and Energy Dispersive X-ray Spectroscopy (SEM-EDS), as well as Surface Area Analyzer (SAA).

2.3 Biodiesel Production

The transesterification reaction required mixing 75 mL of used cooking oil with methanol at mole ratios of 1:3, 1:6, and 1:9, using 3% NiO catalyst by weight of the oil. The mixture was refluxed at 60°C for 4 hours at a stirring speed of 500 rpm. After the process, the biodiesel layer was separated and washed using warm water (Monika et al., 2023).

Methyl ester quality test, with density tests (picnometer), acid number, iodine, saponium, and cetane, and the methyl ester content was analyzed with GC-MS.

3. RESULTS AND DISCUSSION

3.1 Synthesis and Characterization of NiO Nanoparticle Catalysts

The synthesis of NiO nanocrystals through the sol-gel route using nickel chloride hexahydrate as a precursor offers an effective and straightforward method for producing nanoscale oxides with controlled morphology. In the presence of NaOH, $Ni(OH)_2$ from $NiCl_2{\cdot}6H_2O$ underwent hydroxylation of Ni^{2+} ions, forming insoluble hydroxide intermediates that served as essential precursors for oxide formation. Calcination at 450°C for 1 hour converted $Ni(OH)_2$ undergoes thermal decomposition to NiO, releasing water as a byproduct. The black coloration of the product showed successful conversion to NiO, consistent with previous results (Purkan et al., 2021; Shamim et al., 2019).

The calcination temperature critically determined the crystallinity, particle size, and surface area of the resulting NiO. At

Table 1. Catalyst Characterization with SAA

Sample	Surface Area (m^2/g)	Volume @STP (cc/g)	Pore Size (nm)
NiO	489.260	0.43615	1.7829

450°C, the thermal energy was sufficient to induce complete dehydration and crystallization without excessive grain growth. Literature suggested that calcination below 400°C often resulted in incomplete conversion, leaving residual hydroxide phases that compromise catalytic activity, while temperatures above 600°C led to particle agglomeration, reducing the active surface area crucial for catalytic processes. Consequently, maintaining calcination at 450°C offered an optimal compromise between structural integrity and surface reactivity.

In this study, the XRD pattern showed sharp diffraction peaks corresponding to the cubic NiO phase (JCPDS No. 47-1049), with the most intense reflection at $2\theta \approx 43.47°$ (Figure 2). In addition, the absence of additional peaks from $Ni(OH)_2$ or chloride impurities confirmed the complete transformation and high phase purity. The selected calcination temperature (450°C) provided a balance between crystallinity and nanoscale particle retention temperatures below 400°C. This led to incomplete conversion, while those above 600 °C typically promoted particle sintering and surface area loss (Fatimah et al., 2023; Nashim et al., 2024).

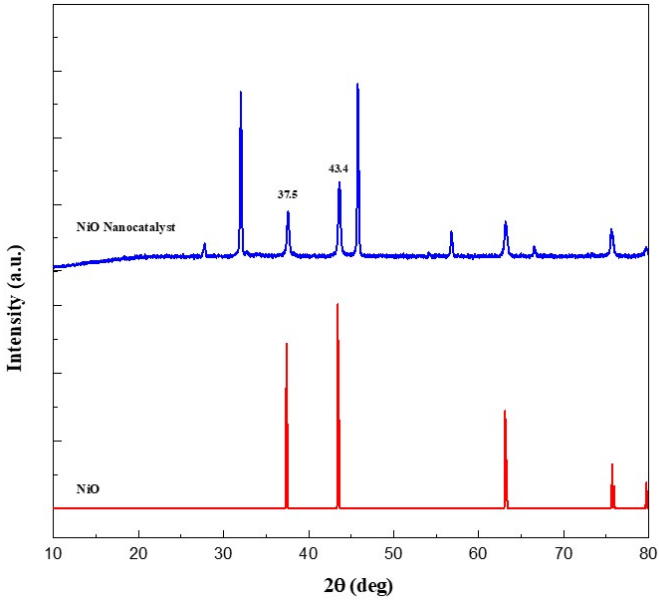

Figure 2. NiO Nanocatalyst XRD Diffraction Pattern Using the Match Application

Characterization of the morphology and chemical composition of NiO nanoparticles that functioned as heterogeneous catalysts was carried out using the SEM-EDS instrument. This analysis aimed to understand the surface structure as well as the distribution of elements in the catalyst (Dong et al., 2025). In Figure 3, it was observed that NiO nanoparticles had a uniform morphology with a spherical shape, a rough or porous surface, and a particle size distribution from SEM analysis showed an average diameter in the nanometer range, showing good size uniformity (Figure 4). The EDS spectrum shown in Figure 5, confirmed the presence of elements Ni and O evenly distributed on the surface of the sample, with the percentage of atoms in the composition of NiO nanoparticles being Ni (47.7 %) and O (20.9%). Such surface texturing enhanced the number of active sites available for catalytic reactions. In addition, the EDS spectra confirmed that Ni and O were the only major elements present, validating the formation of pure NiO without residual contaminants. The results of this analysis were consistent with the NiO morphology obtained from nickel sulfate solutions (Ingalagondi et al., 2025; Roshid et al., 2025).

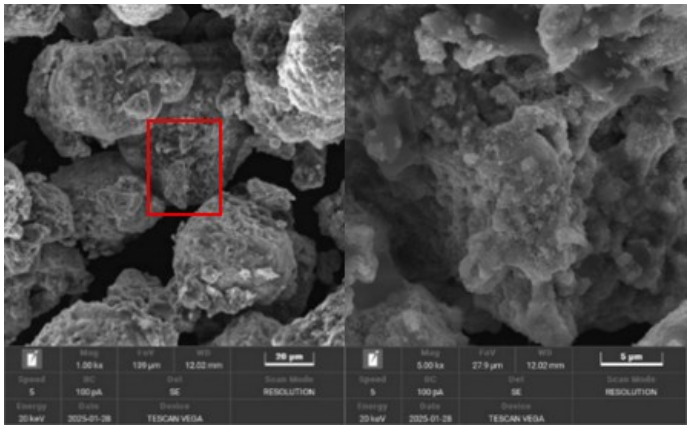

Figure 3. Surface Morphology of NiO Nanoparticles with Magnification of 1000× (Left) and 5000× (Right)

Particle size, surface area, and pore size of NiO nanoparticles were analyzed using PSA and SAA, as shown in Table 1. The PSA results in Figure 6 showed that the NiO nanoparticle size distribution was 39.02 with an intensity of 39.49 with a Polydispersity Index (PI) of 0.010. Figure 6 showed a very uniform particle size distribution and was included in the monodisperse category, because PI <0.1. This suggested that the synthesis process successfully created particles of homogeneous size without significant agglomeration. The particle size distribution could be seen from the values of D10, D50, and D90, which were 32.45 nm, 37.00 nm, and 42.28 nm, showing a narrow size distribution.

NiO nanoparticles derived from $NiCl_2{\cdot}6H_2O$ precursors were characterized using SAA instruments to determine their active surface area. Based on Figure 7, the nitrogen adsorption-desorption isothermal curve showed type III characteristics

Table 2. Results of Biodiesel Characterization

Parameters	Unit	SNI 7182:2015	Biodiesel Produced		
			Mole Ratio 3:1	Mole Ratio 6:1	Mole Ratio 9:1
Yields	%	-	44	45	97.79
Density	g/mol	0.85–0.89	0.86	0.89	0.89
Number of Acids	mg KOH/g	<0.5	0.52	0.4	0.48
Number of Sabotages	mg KOH/g	-	45.75	114.07	97.24
Number of Iodine	mg I_2/g	<115	93.13	67.73	76.2
Number of Cetane	-	>51	114.86	76.87	82.98

Table 3. Methyl Ester Content of Biodiesel Analysis Using GC-MS

Peak of the Spectrum	Retention Time (minutes)	Area (%)	Methyl Ester Compounds	Molecular Formula
1	25.870	54.48	Methyl Octadeconate	$C_{19}H_{36}O_2$
2	21.441	31.72	Methyl Eicosanoate	$C_{21}H_{42}O_2$
3	26.155	7.52	Methyl Stearate	$C_{19}H_{38}O_2$
4	18.088	1.79	Methyl Myristate	$C_{15}H_{30}O_2$
5	24.916	1.37	Methyl Oleate	$C_{19}H_{34}O_2$

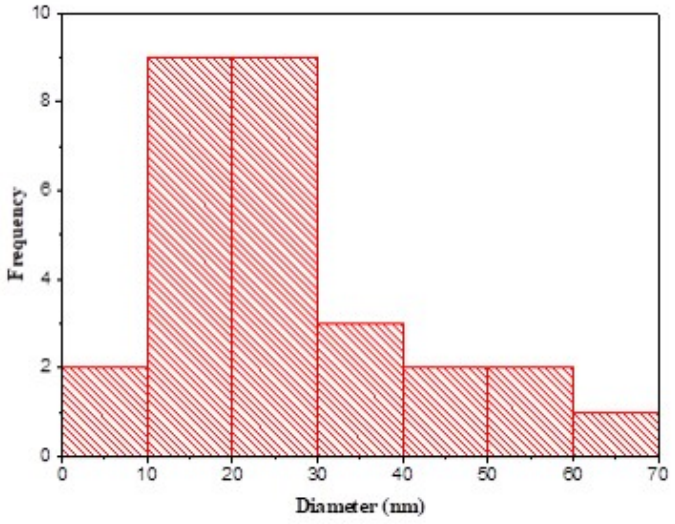

Figure 4. Particle Size Distribution from SEM Data

according to the IUPAC classification, which is characterized by the shape of the curve that was convex to the relative pressure axis (P/P_o) in the absence of a clear turning point (Xu et al., 2025). At the beginning of the curve (P/P_o <0.1), the volume of adsorbed gas increased slowly, while at relatively high pressure (P/P_o >0.9), an increase in the volume of adsorbate was observed. This showed the formation of a multilayer, with the interaction between adsorbate being more dominant than the interaction between adsorbate and adsorbent (Akhtar et al., 2024; Dhaouadi et al., 2024).

The average surface area test results of NiO nanoparticles were recorded at 489.260 m^2/g, which was higher than the previous study of 342 m^2/g for NiO_6 samples. This difference was due to variations in the structure and properties of the samples used in the experiment (Cremer et al., 2023; Wang et al., 2024). The type III isotherm pattern suggested weak adsorbate-adsorbent interactions and the presence of mesoporous structures. A high surface area directly correlated with greater catalytic efficiency since more active NiO sites were exposed for methanol and triglyceride interactions during transesterification.

3.2 Application of NiO Nanoparticle Catalyst in Biodiesel Production

The transesterification of used household cooking oil using NiO nanocatalysts showed the feasibility of converting waste feedstock into biodiesel through a sustainable and heterogeneous catalytic process. The pretreatment stage, which included filtration and neutralization, effectively reduced the free fatty acid (FFA) level to 0.31%. Since this value was below the 1% threshold, the direct base-catalyzed transesterification proceeded without the risk of excessive soap formation. This was consistent with previous results by Susilowati et al. (2019), showing that oils with low FFA content minimized catalyst deactivation and improved biodiesel yield.

Heating the oil to 100 to 110°C for 1.5 hours before reaction was carried out to remove residual moisture to below 0.05% (w/w). This step was crucial, as the presence of water promoted saponification and glycerol emulsification, thereby reducing product purity. The control of water content enhanced reaction efficiency and the phase separation of biodiesel and glycerol, a common challenge in heterogeneous systems.

The catalytic activity of NiO at 3 wt% loading and varying methanol-to-oil molar ratios (1:3, 1:6, and 1:9) provided insight into the balance between reactant concentration and active site availability. At lower methanol ratios, the conversion was limited by equilibrium constraints, while excessive methanol (e.g., 1:9) could dilute reactants and complicate glyc-

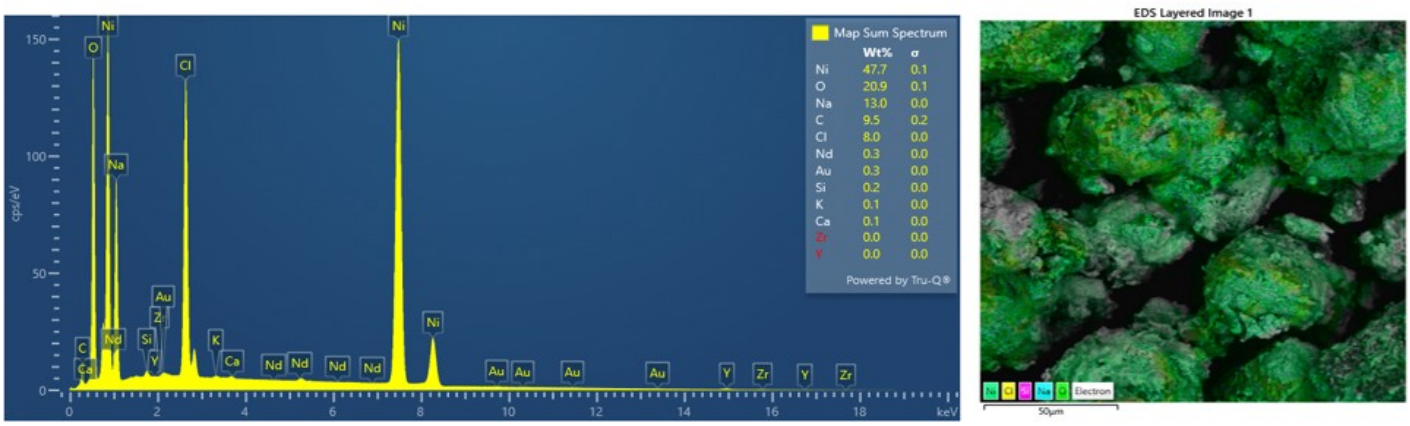

Figure 5. EDS NiO Nanoparticles

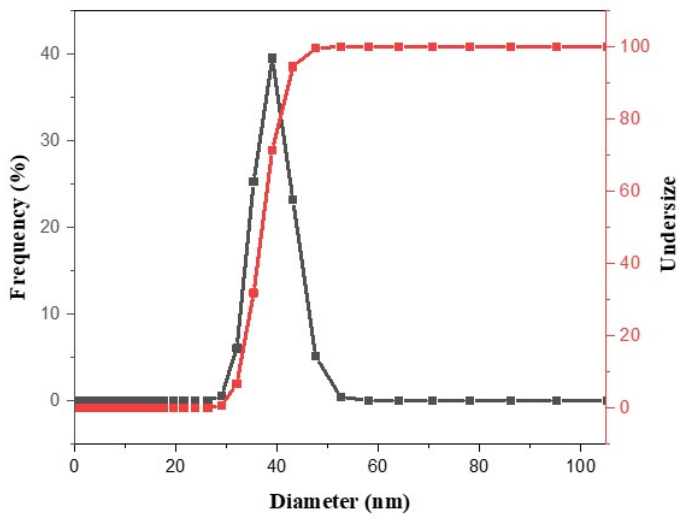

Figure 6. Size Distribution of NiO Nanoparticles Using PSA

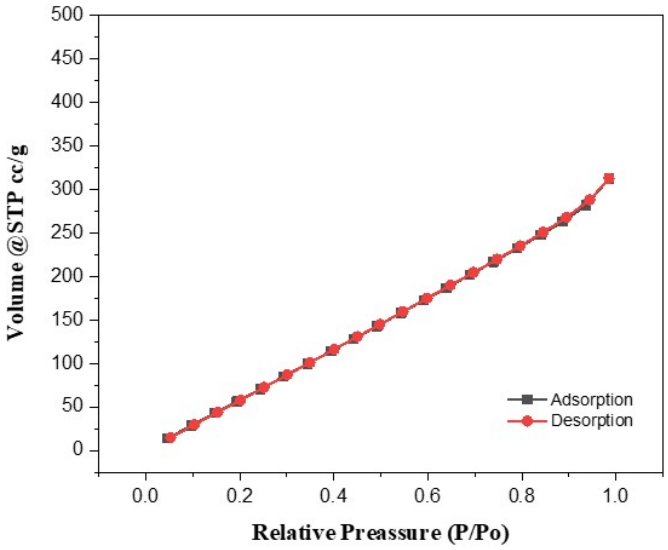

Figure 7. Adsorption-Desorption Curve of NiO Nanoparticles

erol separation. The reflux conditions at 60°C for 4 hours corresponded to the optimal operational range for metal oxide catalysts such as NiO, MgO, and CaO, as supported by previous studies (Purkan et al., 2021; Shamim et al., 2019). These conditions ensured adequate activation of methanol molecules and facilitated adsorption–desorption cycles at the catalyst surface (Figure 8).

After the reflux process, the mixture was placed into a separation funnel to separate the 3 layers. The top layer was methyl ester (biodiesel), the bottom layer was glycerol, and the third layer was the catalyst. This separation occurred due to differences in density, namely, biodiesel, which was lighter (850-890 kg/m^3) than glycerol (1260 kg/m^3). After that, the methyl ester was washed with warm water until the water was clear again. The purpose of this washing was to prevent the formation of emulsions and avoid saturated methyl ester deposits (Huda et al., 2024; Maheshwari et al., 2022). In this study, the final result of this process was in the form of clear yellow biodiesel.

This study aimed to evaluate the efficiency and economic aspects of biodiesel production by measuring the yield of methyl ester. Variations in the ratio of oil moles to methanol had a significant effect on production yields. The 1:9 ratio had the highest yield of 97.79%, while the 1:3 ratio exhibited the lowest yield of 44%. Several studies supported that the ideal ratio was between 1:9 and 1:12. In addition, the optimal temperature was at 60°C, and the addition of a 3% could increase yields by up to 90%. However, when the ratio was too high (>15:1),product separation became difficult, and refining costs increased (Ali et al., 2025; Elfaleh et al., 2023).

The quality of methyl esters was tested quantitatively through various parameters. In addition, the methyl ester density was in the range of 0.86 to 0.89 g/mL and had met the SNI 7182:2015 standard. The number of soaps showed values between 45.75 to 114.07 mg KOH/g, still within safe limits based on ASTM D6751. Iodine number was in the range of

Table 4. Comparison of NiO Nanocatalyst Performance in Biodiesel Production with Previous Studies

Catalyst Type	Feed stock	Synthesis Method	Optimum Methanol: Oil Ratio	Catalyst Loading (% w/w)	Reaction Temperature (°C)	Yield (%)	Specific Surface Area (m^2/g)	Remarks / Advantages	Reference
NiO (This study)	Used cooking oil	Sol–gel	1:9	3%	60	97.79	489.26	High surface area, uniform nanostructure, monodisperse particles, meets SNI & APEC standards	Present study
CaO	Waste cooking oil	Calcination of eggshells	1:12	5%	65	89.5	120.4	Moderate yield, requires higher temperature, catalyst deactivates after reuse	(Huda et al., 2024)
ZnO	Palm oil	Precipitation	1:9	4%	60	82.3	215.6	Good conversion, but lower thermal stability	(Maheshwari et al., 2022)
TiO_2	Jatropha oil	Sol–gel	1:6	3%	65	76.8	142.8	Low yield, sensitive to water content	(Elfaleh et al., 2023)
NiO	Soybean oil	Co-precipitation	1:9	3%	60	91.6	342.0	Moderate surface area, less uniform particle size	(Wang et al., 2024)

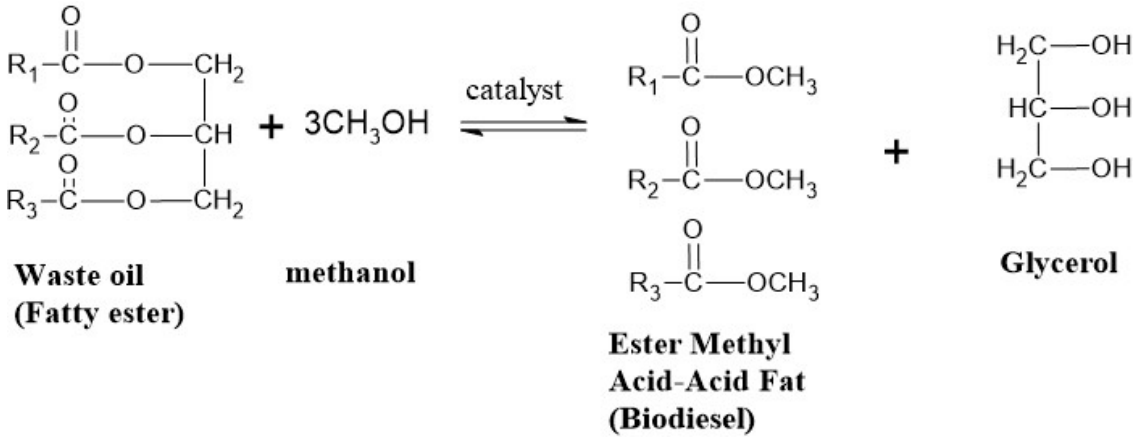

Figure 8. General Schematic Representation of the Transesterification Reaction

67.73 to 93.13 mg/g, which reflected the stability of biodiesel against oxidation and meets the maximum standard of 115 mg/g. The setane number, as an indicator of combustion performance, was in the range of 76.87-114.86 and far exceeded the minimum standard of 51. Meanwhile, the acid number was at 0.40-0.52 mg KOH/g, according to the national standard maximum limit of 0.5 mg KOH/g, in Table 2 characterisation of biodiesel.

Qualitative analysis using GC-MS showed 5 dominant methyl ester compounds found in the samples, namely methyl octadeanoate, methyl eikosan oat, methyl sterate, methyl myristat, and methyl oleate (Figure 9). All of these compounds had a C15-C21 carbon chain length and were compliant with APEC standards. Based on the results of this analysis, biodiesel produced from used cooking oil met national quality standards (SNI) and was suitable for use as an alternative fuel, as shown in the GC-MS analysis results in Table 3 .

NiO nanoparticles were stable and could be reused as a recy-

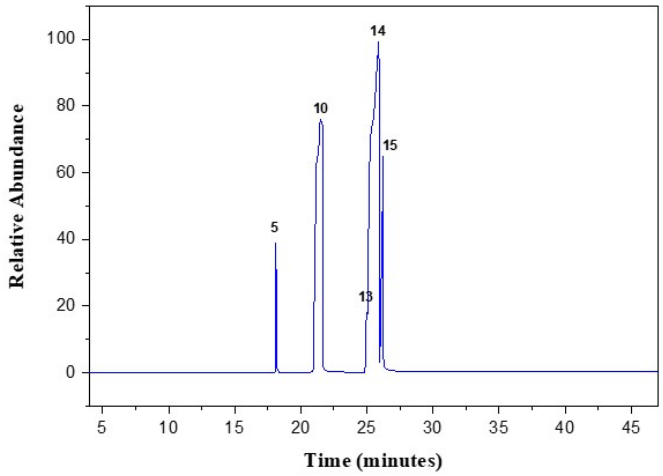

Figure 9. GC-MS Chromatogram of Biodiesel Products Resulting from the Transesterification Reaction of Used Cooking Oil and Methanol Using NiO Nanoparticles Catalyst

clable catalyst. After the transesterification reaction, the catalyst maintained its performance with over 90% of the initial activity retained after 3 consecutive uses. This result showed that the NiO nanoparticles possessed good thermal and structural stability, showing no noticeable deactivation or agglomeration. In addition, it could be effectively reused as a durable and efficient heterogeneous catalyst for biodiesel production, as shown in Table 4, comparing the results of this study with previous studies. The reusability of NiO nanoparticles emphasized their economic and environmental advantages compared to homogeneous catalysts, which were difficult to recover and generate wastewater.

The combination of nanometer-scale particle size, high surface area, uniform morphology, and robust structural integrity collectively contributed to the superior catalytic activity of NiO nanoparticles. These results not only confirmed the feasibility of using sol–gel-synthesized NiO as a sustainable heterogeneous catalyst but also provided a foundation for optimizing reaction kinetics, scaling up production, and enhancing the circular utilization of waste cooking oil in biodiesel synthesis.

4. CONCLUSIONS

In conclusion, NiO nanoparticles synthesized by the sol–gel method successfully yield FCC cubic particles with an average size of 37 nm (PI = 0.010), exhibiting a spherical morphology with micropores (~1.8 nm) and a large surface area (489.26 m^2/g). The atomic composition is uniform atomic composition (Ni 47.7%, O 20.9%). When used as a heterogeneous catalyst for the transesterification of used cooking oil, the best conditions are found at a methanol:oil mole ratio of 9:1.This resulted in a high methyl ester yield of 97.79%, which meets all SNI 7182:2015 parameters (density, acid number, iodine, cetane) and C15-C21 carbon chain profile. The performance of this catalyst is comparable to or even exceeds the previous literature on NiO as a catalyst for successfully converting cordia dichotoma seed oil as a raw material by 94%. These results confirm that NiO nanoparticles exhibit enormous potential as an environmentally friendly catalyst in biodiesel production.

5. ACKNOWLEDGMENT

The authors are grateful to the Chemistry Laboratory of FMIPA UNM, the Chemical Engineering Laboratory of PNUP, and the Chemistry Laboratory of Hasanuddin University for their facilities and technical support during this study.

REFERENCES

Akhtar, M. S., S. Ali, and W. Zaman (2024). Innovative Adsorbents for Pollutant Removal: Exploring the Latest Research and Applications. *Molecules*, **29**(18); 1–37

Al-Fakeh, M. S., R. O. Alsaedi, M. Aldoghaim, A. B. M. Ibrahim, and A. M. Mostafa (2025). Nickel Oxide Nanoparticles Derived from Coordination Polymer of PVA and Aminobenzoic Acid Derivative: Synthesis, Characterization and Antimicrobial Activity. *Polymers*, **17**(3); 301

Ali, A., S. Afrin, A. H. Asif, Y. Arafat, and M. R. Azhar (2025). A Comprehensive Review on the Recovery of Lithium from Lithium-Ion Batteries and Spodumene. *Journal of Environmental Management*, **391**; 126512

Anekwe, I. M. S., S. O. Akpasi, E. K. Tetteh, A. S. Joel, S. I. Mustapha, and Y. M. Isa (2025). Progress in Heterogeneous Catalysis for Renewable Energy and Petrochemical Production from Biomass. *Fuel Processing Technology*, **275**; 108267

Bikbashev, A., T. Stryšovský, M. Kajabová, Z. Kovářová, R. Prucek, A. Panáček, J. Kašlík, T. Fodor, C. Cserháti, Z. Erdélyi, and L. Kvítek (2024). NiO Nano- and Microparticles Prepared by Solvothermal Method: Amazing Catalysts for CO_2 Methanation. *Molecules*, **29**(20); 1–19

Borlaf, M. and R. Moreno (2021). Colloidal Sol-Gel: A Powerful Low-Temperature Aqueous Synthesis Route of Nanosized Powders and Suspensions. *Open Ceramics*, **8**; 100200

Buchori, L., Widayat, N. Ngadi, Hadiyanto, and N. Okvitarini (2024). Preparation of KI/ KIO_3 /Methoxide Kaolin Catalyst and Performance Test of Catalysis in Biodiesel Production. *Science and Technology Indonesia*, **9**(2); 359–370

Cremer, G., S. Danthine, V. Van Hoed, A. Dombree, A. S. Laveaux, C. Damblon, R. Karoui, and C. Blecker (2023). Variability in the Substitution Pattern of Hydroxypropyl Cellulose Affects Its Physico-Chemical Properties. *Heliyon*, **9**(2); e13604

Dey, S. and N. S. Mehta (2020). Oxidation of Carbon Monoxide over Various Nickel Oxide Catalysts in Different Conditions: A Review. *Chemical Engineering Journal Advances*, **1**; 100008

Dhaouadi, F., F. Aouaini, B. Basha, A. Bonilla-Petriciolet, J. Georgin, and A. Ben Lamine (2024). Evaluation and Analysis of the Adsorption Mechanism of Three Emerging Pharmaceutical Pollutants on a Phosphorised Carbon-Based Adsorbent: Application of Advanced Analytical Mod-

els to Overcome the Limitation of Classical Models. *Heliyon*, **10**(14); e34788

Dong, D., Y. Li, M. Liu, B. Lu, X. Yan, Z. Deng, C. Chang, and K. Zhou (2025). Geometric Structure-Dependent Catalyst Performance in CH_4 Reforming Using Ni-Based Catalysts. *Catalysts*, **15**(3); 200

Elfaleh, I., F. Abbassi, M. Habibi, F. Ahmad, M. Guedri, M. Nasri, and C. Garnier (2023). A Comprehensive Review of Natural Fibers and Their Composites: An Eco-Friendly Alternative to Conventional Materials. *Results in Engineering*, **19**; 101271

Fatimah, I., R. Z. Sulistyowati, A. Wijayana, G. Purwiandono, and S. Sagadevan (2023). Z-Scheme NiO/g-C3N4 Nanocomposites Prepared Using Phyto-Mediated Nickel Nanoparticles for the Efficient Photocatalytic Degradation. *Heliyon*, **9**(5); e16232

Hasson, S. S. and A. M. A. Alsammarraie (2022). Synthesis of Nickel Oxide Nanoparticles by Sol-Gel Method. *International Journal of Health Sciences*, **6**; 48938–48947

Huda, M. S., M. Odegaard, N. Chandra Sarker, D. C. Webster, and E. Monono (2024). Enhancing Recovery Yield of Vegetable Oil Methyl Ester for Bioresin Production: A Comparison Study Using Acid Neutralization. *ChemEngineering*, **8**(1); 16

Ingalagondi, P. K., M. S. Sannaikar, K. Mruthunjaya, and N. C. Horti (2025). Optical and Antibacterial Properties of Nickel Oxide (NiO) Nanoparticles: Effect of Annealing Temperature. *Results in Surfaces and Interfaces*, **19**; 100571

Maheshwari, P., M. B. Haider, M. Yusuf, J. J. Klemeš, A. Bokhari, M. Beg, A. Al-Othman, R. Kumar, and A. K. Jaiswal (2022). A Review on Latest Trends in Cleaner Biodiesel Production: Role of Feedstock, Production Methods, and Catalysts. *Journal of Cleaner Production*, **355**; 131588

Monika, S. Banga, and V. V. Pathak (2023). Biodiesel Production from Waste Cooking Oil: A Comprehensive Review on the Application of Heterogeneous Catalysts. *Energy Nexus*, **10**; 100209

Naseef, H. H. and R. H. Tulaimat (2025). Transesterification and Esterification for Biodiesel Production: A Comprehensive Review of Catalysts and Palm Oil Feedstocks. *Energy Conversion and Management: X*, **26**; 100931

Nashim, A., S. Pany, and K. Parida (2024). Effect of Synthesis Methods on the Activity of NiO/ Co_3O_4 as an Electrode Material for Supercapacitor: In the Light of X-Ray Diffraction Study. *RSC Advances*, **14**(1); 233–244

Oladipo, A., O. Ejeromedoghene, O. K. Olaseinde, V. Enwemiwe, and K. A. Samson (2025). Waste-to-Fuel: The Potentials of Waste Hard Nutshell Oil and Biowaste Heterogeneous Catalysts for Biodiesel Production. *Next Sustainability*, **6**; 100145

Pratiwi, N., S. E. Putri, Y. Shinta, A. I. Batara, D. E. Pratiwi, A. Rahman, N. Ahmad, and H. Heryanto (2024). Synthesis and Characterization of Renewable Heterogeneous Catalyst ZnO Supported Biogenic Silica from Pineapple Leaves Ash for Sustainable Biodiesel Conversion. *Karbala International Journal of Modern Science*, **10**(1); 99–117

Purkan, P., A. Safa, A. Abdulloh, A. Baktir, R. Arissirajudin, H. Hermansyah, and S. W. Kim (2021). In-Situ Biodiesel Synthesis from Microalgae Nannochloropsis Oculata Using NiO Nanocatalyst. *Rasayan Journal of Chemistry*, **14**(3); 2097–2103

Roshid, M. H., M. S. Alam, K. A. Ibn Amin, F. K. Ferdousi, M. H. Rahman, and S. Islam (2025). Green Synthesis of Nickel Oxide Nanoparticles Using Lagerstroemia Speciosa, Bombax Ceiba, and Piper Chaba Extracts and Evaluating Their Potential Antioxidant, Antidiabetic and Antibacterial Properties. *Heliyon*, **11**(6); e42953

Sales, H. B., R. R. Menezes, G. A. Neves, J. J. N. de Souza, J. M. Ferreira, L. Chantelle, A. L. M. de Oliveira, and H. d. L. Lira (2020). Development of Sustainable Heterogeneous Catalysts for the Photocatalytic Treatment of Effluents. *Sustainability*, **12**(18); 7393

Saputra, K., M. Masruroh, H. Susanto, and R. Apsari (2024). Tapping Into the Power of Sol-Gel Method for Enhanced Antimicrobial Activity of Titania Nanoparticles. *Science and Technology Indonesia*, **9**(3); 546–555

Shamim, A., Z. Ahmad, S. Mahmood, U. Ali, T. Mahmood, and Z. A. Nizami (2019). Synthesis of Nickel Nanoparticles by Sol-Gel Method and Their Characterization. *Open Journal of Chemistry*, **2**(1); 16–20

Susilowati, E., A. Hasan, and A. Syarif (2019). Free Fatty Acid Reduction in a Waste Cooking Oil as a Raw Material for Biodiesel With Activated Coal Ash Adsorbent. *Journal of Physics: Conference Series*, **1167**(1); 012035

Wan Osman, W. N. A., M. H. Rosli, W. N. A. Mazli, and S. Samsuri (2024). Comparative Review of Biodiesel Production and Purification. *Carbon Capture Science and Technology*, **13**; 100264

Wang, Y., X. Ou, Q. A. Al-Maqtari, H. J. He, and N. Othman (2024). Evaluation of Amylose Content: Structural and Functional Properties, Analytical Techniques, and Future Prospects. *Food Chemistry: X*, **24**; 101830

Xu, G., M. He, L. He, Y. Chen, L. Duan, and W. Jiao (2025). A Study on the Relationship Between the Pore Characteristics of High-Performance Self-Compacting Concrete (HPSCC) Based on Fractal Theory and the Function of the Water–Binder Ratio (W/C). *Journal of Composites Science*, **9**(2); 66

